STAND3 Particle Detector Response Function, Purity, Efficiency, and Response to Charged and Neutral CR Species

T. Karapetyan and G. Hovsepyan

A. I. Alikhanyan National Science Laboratory (Yerevan Physics Institute), Yerevan, Armenia 36

E mail: ktigran79@gmail.com

Accepted: 08 November 2025

Abstract: This study presents a detailed analysis of the STAND3 detector response functions, detection efficiencies, and purities for various secondary cosmic ray species—neutrons, protons, muons, electrons, positrons, and gamma rays—based on GEANT4 simulations using realistic atmospheric spectra from EXPACS. The STAND3 detector, operated at the Aragats Cosmic Ray Station (3200 m a.s.l.), is the main instrument for detecting Thunderstorm Ground Enhancements (TGEs) and investigating the energetic electron component of these events.

Special attention is given to coincidence configurations 1100, 1110, and 1111, which correspond to energy thresholds for electrons of approximately > 20 MeV, > 30 MeV, and > 40 MeV, respectively. Simulation results demonstrate that STAND3 achieves high detection efficiency (above 70-80%) and purity (above 70%) for energetic electrons and positrons in the 1110 and 1111 coincidences, while lower coincidences such as 1100 remain effective for detecting softer electron components. By this way these coincidences allow for precise separation and spectral characterization of TGE-related electrons. These findings confirm that STAND3 provides reliable, energy-resolved, and high-purity measurements of TGE electrons, making it a key detector for continuous 24/7 monitoring of thunderstorm-related particle enhancements and for studying high-energy atmospheric processes.

Key words: STAND3 detector response functions, detection efficiencies

Introduction

Radiation on Earth's surface has been measured for over a century using various particle detectors. These detectors have evolved from electroscopes to sophisticated, massive detectors like the Large Hadron Collider (LHC). Here we will concentrate on particle detectors operated at Aragats Cosmic Ray Observatory [1] operated by the Cosmic Ray Division (CRD) of the Yerevan Physics Institute (YerPhI) [2]. Various types of particle detectors record different kinds of cosmic rays. To make physical inferences using measured data from a detector, we need to calculate the detector response. In other words, to calculate the expected measurement of various particles with different energies. Then, using the detector response, we demonstrate that we have measured a genuine signal, possibly establishing a new physical process. The "STAND3" detector consists of four layers of 3-cm-thick, 1-m² sensitive area scintillators stacked horizontally, as shown in Fig. 1. Light from the scintillator, transmitted through optical spectrum-shifter fibers, is reradiated to the long-wavelength region and directed to the photomultiplier (PMT FEU-115M). Maximum luminescence occurs at a wavelength of 420 nm, with a luminescence time of about 2.3 ns. The STAND3 detector is calibrated by adjusting the high voltage applied to the PMT and setting the shaper-discriminator thresholds. The discrimination level is selected to detect signals effectively while minimizing the suppression of photomultiplier noise as much as possible. Coincidences of signals from all four layers enable the selection of electrons with energy thresholds ranging from 10 MeV ("1000" coincidence, signal only in the top layer) to more than 40 MeV ("1111" coincidence, signals in all layers).

DOI: 10.31401/SunGeo.2022.02.01

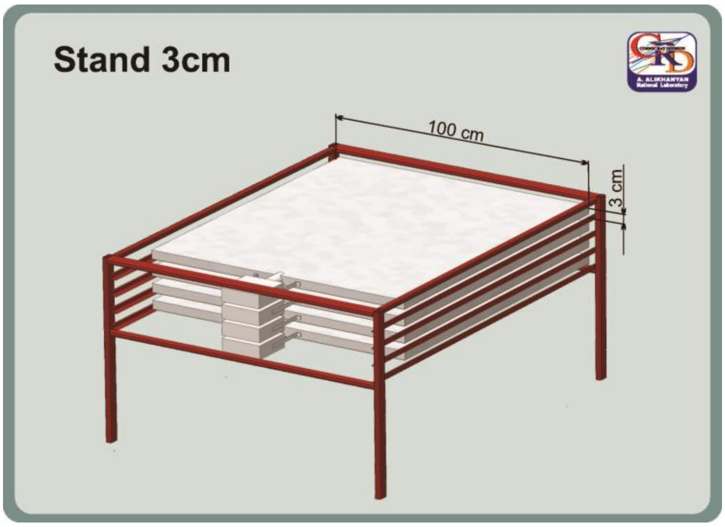

Figure 1. STAN3 detector measuring charged and neutral species of secondary cosmic rays

The detector's count rate is influenced by various factors, such as its size, location, and registration efficiency. Atmospheric pressure, temperature, NSEF, geomagnetic field, and solar wind also affect the count rate. Additionally, the count rate may be influenced by power supply oscillations, diurnal and seasonal changes, and the randomness of physical processes used for particle detection, such as PMT noise. To derive parameters with physical meaning, we must deconvolute the measured count rate to make it independent of the detector's specific characteristics, estimate different particle fluxes and energy spectra as they existed before entering the detector, and assess measurement errors. Understanding how the particle detector registers elementary particles is essential to ensure accurate results. Without understanding the detector's response, particle flux measurements will be arbitrary, and any physical inference based on them will be unreliable. This is known as the direct problem of CR. The best way to address this is through particle beam calibrations on artificial accelerators; however, this option is not always available. Alternatively, we can use CR flux generators, such as EXPACS [3], to obtain flux data for all CR species across all latitudes, longitudes, and altitudes, combined with the GEANT4 code [4] for particle tracking. However, it's important to remember that simplifying the model will affect the recovered particle fluxes and may impact the reliability of any physical inferences made. The tables show the purity of the STEND3 detector obtained using EXPACS and GEANT4 packages. EXPACS provides the flux of all cosmic ray species at the observation point, while GEANT4 tracks all particles entering the detector setup. To determine the particle frequencies, we need to solve the inverse cosmic ray problem by using the measured composition to recover the true one.

Purity and Efficiency in Secondary Cosmic Ray Detection

In this study, by using GEANT4 simulation package [5] we simulate the fluxes of secondary cosmic ray particles — such as neutrons, protons, muons, electrons, positrons and gamma rays — based on approximate atmospheric fluxes provided by the EXPACS (http://phits.jaea.go.jp/expacs/ Excel-based Program for calculating Atmospheric Cosmic-ray secondaries Spectrum) calculator for a given location and above Earth's surface. The performance of the GEANT4 simulated detector system is evaluated using two key metrics: efficiency and purity.

Detection Efficiency: refers to the fraction of any secondary particles hitting the detector that successfully interact with the detector and produce a measurable signal. It is defined as:

Efficiency=Nregistered/Nhitted

A high efficiency indicates that the detector is effective at capturing and recording the particles it is intended to measure.

Purity, on the other hand, quantifies how many of the recorded signals actually originate from desired secondary cosmic ray particle, rather than from other particles. It is defined as:

Purity=Ntrue /Ntotal

The purity tables show the types of registered particles by (%) of total flux. The sum of each row equals 100%. From the registered count rate of detector layers, or coincidences, we cannot distinguish the contributions of different particle types. Using the GEANT4 simulations we can get insight obtain such information, which has been implemented in this work. Maintaining high purity is essential to ensure that the collected data accurately represents the physical processes under investigation, without significant contamination from unrelated signals.

By evaluating both purity and efficiency, we can assess the reliability of the detector configuration and optimize its design for cosmic ray monitoring under real environmental conditions.

The GEANT4 simulations were made by using the following conditions:

1. The particles are dropped at a distance of 10 cm from the center of the detector.
2. The zenith angles are simulated according to Cos2.5(θ) and azimuth-uniform in 0 - 2π.
3. The energy range of Secondary Cosmic Rays (SCR) is 1.13 MeV to 1130 MeV.
4. As the GEANT4 input, spectra of secondary cosmic rays, calculated by EXPACS, are used at the incident on the top of the detector or building where the detector is located. These spectra provide a realistic approximation of particle fluxes at the observation level of the detector sites.
5. All particles are then tracked through the detector according to the GEANT4 geometry, and all interactions with the sensitive volumes are analyzed and recorded.
6. For almost all species of secondary cosmic rays (electrons, positrons, positive and negative muons, gamma rays, protons, and neutrons), 10000 events were simulated for each.

The tables below contain information about registration efficiencies and purities for secondary CRs for the STAND3 detector located at Aragats high-altitude research station.

Information is crucial for understanding of composition and energies of short particle bursts. For instance, from Table 16, we can see that coincidence 1111 (signals in all four layers of the detector) is associated with high confidence with the registration of an electron with an energy greater than 45 MeV (if we register thunderstorm ground enhancement – TGE). The purity of the "1111" selection is as follows: neutrons (0%), protons (0%), muons (sum of mu+ and mu-) ~ 39%, sum of electrons and positrons ~60%, and gamma rays ~ 1%. Muon flux during TGE didn't increase, thus we can attribute 99% of the flux to high-energy electrons.

For minimum-ionizing particles for muons in the relativistic range, the mean energy loss in plastic scintillator is roughly and equal to ≈2 MeV per g/cm2, so a muon passing through all 4 layers ("1111" coincidence, signals in all layers) means deposits ~25 MeV in total only in scintillators and by taking into account the steal covers of each scintillator enable the selection of muons with energy thresholds more than 45MeV. The results obtained by GEANT 4 simulation (described above) are in good agreement with the expectation from predefined energy threshold.

Aragats, Armenia, altitude - 3200 m

Table 1. Geometry and materials of the STAND3 detector used in GEANT4 simulations (Aragats Station, 3200 m a.s.l.)

Component	Materials	Thickness (mm)
Roof cover	Iron (Fe)	0.8
Base of the roof cover	Wood (brevno)	10.0
Each plastic scintillator layer (x 4)		
Top cover	Iron (Fe)	0.8mm
Intermediate plate	DVP (karton)	5.0mm
Active volume	Plastic scintillator	30mm
Bottom plate	DVP (karton)	5.0mm
Base cover	Fe	0.8mm

Table 2. STAND3 Aragats, detector N1, efficiency for secondary CRs (%)

Energy (MeV)	neutron	proton	Mu+	Mu-	electron	positron	gamma
1.13	0.33	0	4.42	4.68	0	0	0
1.42	0.47	0	4.56	5.13	0	0	0
1.79	0.49	0	5.86	6.7	0	0	0
2.25	0.83	0	8.24	9.18	0	0	0
2.84	0.96	0	12.9	12.33	0	0	0.03
3.57	2.13	0	20.68	3.89	0	0.02	2.12
4.5	2.93	0	22.66	3.9	0.01	0.06	3.7
5.66	4.37	0	22.48	4.44	0.01	0.15	4.75
7.13	5.12	0	21.92	3.96	2.54	4.62	5.53
8.97	5.6	0	22.65	18.35	40.03	40.26	6.28
11.3	6.65	0	23.09	22.28	76.07	72.84	7.57
14.2	6.14	0	24.34	21.6	89.94	85.85	7.8

17.9	5.84	0	47.1	32.9	94.44	91.06	8.28
22.5	7.44	0.02	90.4	95.12	96.56	93.38	9.59
28.4	8.95	0.02	99.87	99.83	97.79	95.17	9.16
35.7	9.45	0.04	99.83	99.89	98.45	96.42	8.97
45	10.76	0.05	99.93	99.85	98.62	97.22	9.38
56.6	13.06	82.61	99.94	99.97	99.09	97.25	9.27
71.3	14.54	97.63	99.95	99.93	99.29	98.18	9.98
89.7	18.51	98.53	99.97	99.98	99.37	98.36	10.38
113	24.35	98.79	99.99	99.98	99.64	98.92	10.59
142	31.02	98.99	99.97	99.98	99.76	99.06	10.65
179	38.12	99.23	99.98	99.98	99.81	99.53	10.93
225	44.93	99.4	99.99	99.98	99.82	99.27	11.43
284	50.42	99.62	100	100	99.87	99.37	11.6
357	54.65	99.65	99.99	100	99.91	99.58	11.67
450	57.46	99.72	99.99	100	99.88	99.69	11.86
566	62.85	99.76	100	100	99.94	99.67	12.51
713	68.26	99.78	100	100	99.96	99.77	12.1
897	72.15	99.81	100	100	99.97	99.81	12.6
1130	76.57	99.87	100	100	99.96	99.8	11.86

Table 3. STAND3 Aragats, detector N1, purity for secondary CRs (%)

Energy (MeV)	neutron	proton	Mu+	Mu-	electron	positron	gamma
1.13	3.50	0.00	46.87	49.63	0.00	0.00	0.00
1.42	4.63	0.00	44.88	50.49	0.00	0.00	0.00
1.79	3.75	0.00	44.90	51.34	0.00	0.00	0.00
2.25	4.55	0.00	45.15	50.30	0.00	0.00	0.00
2.84	3.66	0.00	49.20	47.03	0.00	0.00	0.11
3.57	7.39	0.00	71.71	13.49	0.00	0.07	7.35
4.5	8.81	0.00	68.13	11.73	0.03	0.18	11.12
5.66	12.07	0.00	62.10	12.27	0.03	0.41	13.12
7.13	11.72	0.00	50.17	9.06	5.81	10.57	12.66
8.97	4.21	0.00	17.01	13.78	30.06	30.23	4.72
11.3	3.19	0.00	11.07	10.69	36.48	34.94	3.63
14.2	2.61	0.00	10.33	9.17	38.16	36.43	3.31
17.9	2.09	0.00	16.84	11.77	33.77	32.57	2.96
22.5	1.90	0.01	23.03	24.23	24.60	23.79	2.44
28.4	2.18	0.00	24.31	24.30	23.81	23.17	2.23
35.7	2.29	0.01	24.17	24.18	23.83	23.34	2.17
45	2.59	0.01	24.03	24.01	23.72	23.38	2.26
56.6	2.61	16.48	19.94	19.95	19.77	19.40	1.85
71.3	2.80	18.79	19.24	19.24	19.11	18.90	1.92
89.7	3.53	18.76	19.04	19.04	18.92	18.73	1.98
113	4.57	18.56	18.79	18.78	18.72	18.58	1.99
142	5.75	18.35	18.53	18.53	18.49	18.36	1.97
179	6.96	18.12	18.26	18.26	18.23	18.18	2.00
225	8.10	17.92	18.02	18.02	17.99	17.89	2.06
284	8.99	17.76	17.83	17.83	17.81	17.72	2.07
357	9.66	17.62	17.68	17.69	17.67	17.61	2.06
450	10.11	17.54	17.59	17.59	17.57	17.53	2.09
566	10.94	17.36	17.40	17.40	17.39	17.34	2.18
713	11.77	17.21	17.25	17.25	17.24	17.21	2.09
897	12.35	17.08	17.11	17.11	17.11	17.08	2.16
1130	13.02	16.98	17.01	17.01	17.00	16.97	2.02

Table 4. STAND3 Aragats, detector N2, efficiency for secondary CRs (%)

Energy (MeV)	neutron	proton	Mu+	Mu-	electron	positron	gamma
1.13	0.14	0	3.21	3.29	0	0	0
1.42	0.19	0	3.38	3.41	0	0	0
1.79	0.33	0	4.11	4.75	0	0	0
2.25	0.35	0	5.62	6.24	0	0	0
2.84	0.62	0	8.78	7.45	0	0	0
3.57	0.42	0	11.96	1.83	0	0.02	0.69
4.5	1.11	0	13.15	1.89	0	0.01	2.87
5.66	2.2	0	13.49	2.25	0.01	0.1	3.43
7.13	2.84	0	13.06	2.01	0.05	0.14	4.57
8.97	3.08	0	13.62	11.14	0.1	0.3	5.72
11.3	3.04	0	13.91	13.85	0.27	0.66	7.25
14.2	3.68	0	15.7	13.26	0.35	0.84	8.15
17.9	2.98	0.01	24.01	15.15	8.47	9.65	9.79
22.5	3.75	0	28.24	27.64	46.67	46.17	12.98
28.4	4.51	0	33.62	32.94	75.54	70.62	14.5
35.7	5.31	0	47.76	37.97	86.26	83.5	15.48
45	6.56	0.02	98.68	99.41	91.5	88.09	17.65
56.6	7.71	0.08	99.93	99.95	93.99	90.59	17.89
71.3	8.72	0.11	99.94	99.9	95.48	93.22	18.82
89.7	9.38	16.01	99.96	99.98	96.72	94.33	19.2
113	11.62	92.86	99.97	99.97	97.7	95.68	19.87
142	15.79	95.16	99.95	99.98	98.22	96.8	20.15
179	21.47	96.15	99.96	99.97	98.69	97.54	20.4
225	27.28	97.08	99.99	99.98	98.74	97.88	21.3
284	33.89	97.79	100	100	99.19	98.09	22.11
357	39.03	98.47	99.99	99.99	99.35	98.6	22.23
450	43.88	98.61	99.99	100	99.37	98.68	22.51
566	49.85	98.96	100	100	99.51	98.96	23.54
713	57.61	99.17	100	100	99.75	99.29	22.65
897	63.97	99.16	100	100	99.76	99.37	23.59
1130	70.63	99.42	100	100	99.82	99.54	23.37

Table 5. STAND3 Aragats, detector N2, purity for secondary CRs (%)

Energy (MeV)	neutron	proton	Mu+	Mu-	electron	positron	gamma
1.13	2.11	0.00	48.34	49.55	0.00	0.00	0.00
1.42	2.72	0.00	48.42	48.85	0.00	0.00	0.00
1.79	3.59	0.00	44.72	51.69	0.00	0.00	0.00
2.25	2.87	0.00	46.03	51.11	0.00	0.00	0.00
2.84	3.68	0.00	52.11	44.21	0.00	0.00	0.00
3.57	2.82	0.00	80.16	12.27	0.00	0.13	4.62
4.5	5.83	0.00	69.10	9.93	0.00	0.05	15.08
5.66	10.24	0.00	62.80	10.47	0.05	0.47	15.97
7.13	12.53	0.00	57.61	8.87	0.22	0.62	20.16
8.97	9.07	0.00	40.11	32.80	0.29	0.88	16.84
11.3	7.80	0.00	35.68	35.53	0.69	1.69	18.60
14.2	8.77	0.00	37.40	31.59	0.83	2.00	19.41
17.9	4.25	0.01	34.27	21.62	12.09	13.77	13.97
22.5	2.27	0.00	17.07	16.71	28.21	27.91	7.85
28.4	1.95	0.00	14.51	14.21	32.60	30.48	6.26
35.7	1.92	0.00	17.29	13.74	31.22	30.22	5.60
45	1.63	0.00	24.55	24.73	22.77	21.92	4.39

56.6	1.88	0.02	24.36	24.37	22.92	22.09	4.36
71.3	2.10	0.03	24.01	24.00	22.94	22.40	4.52
89.7	2.15	3.68	22.95	22.95	22.20	21.66	4.41
113	2.24	17.94	19.31	19.31	18.87	18.48	3.84
142	3.00	18.09	19.00	19.01	18.67	18.40	3.83
179	4.02	18.00	18.71	18.71	18.48	18.26	3.82
225	5.03	17.90	18.44	18.44	18.21	18.05	3.93
284	6.15	17.75	18.15	18.15	18.00	17.80	4.01
357	7.00	17.66	17.93	17.93	17.82	17.68	3.99
450	7.79	17.51	17.76	17.76	17.65	17.53	4.00
566	8.73	17.34	17.52	17.52	17.43	17.34	4.12
713	9.96	17.14	17.29	17.29	17.24	17.16	3.92
897	10.92	16.93	17.07	17.07	17.03	16.96	4.03
1130	11.92	16.77	16.87	16.87	16.84	16.79	3.94

Table 6. STAND3 Aragats, detector N3, efficiency for secondary CRs (%)

Energy (MeV)	neutron	proton	Mu+	Mu-	electron	positron	gamma
1.13	0.09	0	1.48	1.64	0	0	0
1.42	0.09	0	1.64	1.64	0	0	0
1.79	0.18	0	1.9	2.25	0	0	0
2.25	0.24	0	2.64	2.98	0	0	0
2.84	0.39	0	4.05	3.11	0	0	0
3.57	0.36	0	4.87	0.8	0	0.02	0.68
4.5	0.59	0	5.28	0.86	0	0.03	2.14
5.66	0.89	0	5.76	0.83	0	0.07	2.76
7.13	1.62	0	5.25	0.99	0.05	0.15	3.84
8.97	1.78	0	5.89	4.47	0.06	0.22	4.97
11.3	1.83	0	6.11	5.85	0.21	0.39	6.33
14.2	2.36	0	6.53	5.66	0.41	0.85	7.42
17.9	2.11	0	10.26	6.78	0.69	1.22	8.98
22.5	2.56	0	12.59	12.17	1.19	1.98	11.67
28.4	3.45	0	16.18	15.67	8.3	9.66	14.97
35.7	4.05	0.02	23.04	16.35	40.89	41.8	17.15
45	5.32	0.02	33.99	31.76	67.57	64.77	21.02
56.6	6.24	0.05	82.79	81.25	79.59	77.36	22.93
71.3	7.14	0.15	99.9	99.86	87.82	84.04	25.6
89.7	7.48	0.26	99.92	99.97	90.92	88.16	26.99
113	7.92	0.53	99.95	99.96	93.47	90.71	28.08
142	9.22	80.64	99.92	99.94	95.23	93.05	28.27
179	13.99	91.94	99.93	99.96	96.34	94.73	29.39
225	20.22	93.9	99.97	99.98	96.87	95.61	29.54
284	25.86	95.19	100	99.97	97.85	96.46	31.08
357	31.07	96.67	99.98	99.99	98.28	97.18	30.95
450	35.37	97.05	99.99	99.99	98.61	97.44	31.54
566	41.85	97.86	100	100	98.8	98.2	32.94
713	50.1	98.34	100	100	99.26	98.64	32.14
897	58.17	98.2	100	100	99.29	98.82	32.93
1130	65.9	98.83	100	100	99.52	99.11	33.13

Table 7. STAND3 Aragats, detector N3, purity for secondary CRs (%)

Energy (MeV)	neutron	proton	Mu+	Mu-	electron	positron	gamma
1.13	2.80	0.00	46.11	51.09	0.00	0.00	0.00
1.42	2.67	0.00	48.66	48.66	0.00	0.00	0.00

1.79	4.16	0.00	43.88	51.96	0.00	0.00	0.00
2.25	4.10	0.00	45.05	50.85	0.00	0.00	0.00
2.84	5.17	0.00	53.64	41.19	0.00	0.00	0.00
3.57	5.35	0.00	72.36	11.89	0.00	0.30	10.10
4.5	6.63	0.00	59.33	9.66	0.00	0.34	24.04
5.66	8.63	0.00	55.87	8.05	0.00	0.68	26.77
7.13	13.61	0.00	44.12	8.32	0.42	1.26	32.27
8.97	10.24	0.00	33.87	25.70	0.35	1.27	28.58
11.3	8.83	0.00	29.49	28.23	1.01	1.88	30.55
14.2	10.16	0.00	28.11	24.37	1.76	3.66	31.94
17.9	7.02	0.00	34.15	22.57	2.30	4.06	29.89
22.5	6.07	0.00	29.86	28.87	2.82	4.70	27.68
28.4	5.06	0.00	23.71	22.97	12.16	14.16	21.94
35.7	2.83	0.01	16.08	11.41	28.53	29.17	11.97
45	2.37	0.01	15.14	14.15	30.10	28.86	9.37
56.6	1.78	0.01	23.64	23.20	22.73	22.09	6.55
71.3	1.77	0.04	24.70	24.69	21.71	20.78	6.33
89.7	1.81	0.06	24.15	24.16	21.98	21.31	6.52
113	1.88	0.13	23.76	23.76	22.22	21.57	6.68
142	1.82	15.93	19.74	19.74	18.81	18.38	5.58
179	2.66	17.47	18.99	18.99	18.31	18.00	5.58
225	3.77	17.52	18.65	18.65	18.07	17.83	5.51
284	4.73	17.42	18.30	18.30	17.91	17.65	5.69
357	5.61	17.45	18.04	18.04	17.74	17.54	5.59
450	6.32	17.33	17.86	17.86	17.61	17.40	5.63
566	7.35	17.18	17.55	17.55	17.34	17.24	5.78
713	8.66	17.00	17.29	17.29	17.16	17.05	5.56
897	9.90	16.72	17.02	17.02	16.90	16.82	5.61
1130	11.05	16.57	16.76	16.76	16.68	16.62	5.55

Table 8. STAND3 Aragats, detector N4, efficiency for secondary CRs (%)

Energy (MeV)	neutron	proton	Mu+	Mu-	electron	positron	gamma
1.13	0.09	0	0.47	0.35	0	0	0
1.42	0.07	0	0.56	0.5	0	0	0
1.79	0.13	0	0.63	0.49	0	0	0
2.25	0.25	0	0.82	0.71	0	0	0
2.84	0.27	0	1.19	0.83	0	0	0
3.57	0.16	0	1.49	0.34	0	0	0.48
4.5	0.22	0	1.63	0.36	0	0.01	1.95
5.66	0.35	0	1.88	0.46	0.03	0.02	2.81
7.13	0.77	0	1.56	0.42	0.06	0.14	3.67
8.97	0.78	0	1.75	1.28	0.04	0.21	4.34
11.3	0.98	0	1.78	1.69	0.12	0.42	5.48
14.2	1.43	0	1.81	1.49	0.24	0.65	7.33
17.9	1.42	0	3.14	2.26	0.6	1.05	8.67
22.5	1.8	0	4.38	3.65	0.96	1.53	10.13
28.4	2.46	0	5.95	5.48	1.77	2.85	13.01
35.7	2.87	0.01	9.5	6.74	3.95	5.49	15.82
45	3.83	0	15.65	14.35	24.79	26.51	20.74
56.6	4.67	0.04	30.54	25.97	51.52	50.88	24.44
71.3	5.04	0.06	85.17	84.65	70.64	67.54	28.65
89.7	5.33	0.19	99.87	99.95	80.4	77.16	31.76
113	5.96	0.37	99.94	99.96	86.29	83.75	33.95

142	6.58	6.86	99.93	99.94	90.52	87.8	35.78
179	8.12	85.63	99.92	99.95	93.19	91.01	36.69
225	13.74	89.17	99.94	99.97	94.31	92.77	37.48
284	19	91.71	100	99.96	96.05	94.07	38.52
357	24.09	94.46	99.97	99.98	96.76	95.54	39.04
450	28.19	94.95	99.99	99.99	97.43	96.17	39.82
566	34.08	96.11	99.98	100	97.88	97.21	41.45
713	44.18	97.03	99.99	100	98.51	97.7	40.01
897	52.23	97.44	100	100	98.76	98.1	41.3
1130	61.18	97.86	100	100	99.11	98.54	41.65

Table 9. STAND3 Aragats, detector N4, purity for secondary CRs (%)

Energy (MeV)	neutron	proton	Mu+	Mu-	electron	positron	gamma
1.13	9.89	0.00	51.65	38.46	0.00	0.00	0.00
1.42	6.19	0.00	49.56	44.25	0.00	0.00	0.00
1.79	10.40	0.00	50.40	39.20	0.00	0.00	0.00
2.25	14.04	0.00	46.07	39.89	0.00	0.00	0.00
2.84	11.79	0.00	51.97	36.24	0.00	0.00	0.00
3.57	6.48	0.00	60.32	13.77	0.00	0.00	19.43
4.5	5.28	0.00	39.09	8.63	0.00	0.24	46.76
5.66	6.31	0.00	33.87	8.29	0.54	0.36	50.63
7.13	11.63	0.00	23.56	6.34	0.91	2.11	55.44
8.97	9.29	0.00	20.83	15.24	0.48	2.50	51.67
11.3	9.36	0.00	17.00	16.14	1.15	4.01	52.34
14.2	11.04	0.00	13.98	11.51	1.85	5.02	56.60
17.9	8.28	0.00	18.32	13.19	3.50	6.13	50.58
22.5	8.02	0.00	19.51	16.26	4.28	6.82	45.12
28.4	7.80	0.00	18.88	17.39	5.62	9.04	41.28
35.7	6.47	0.02	21.41	15.19	8.90	12.37	35.65
45	3.62	0.00	14.78	13.55	23.42	25.04	19.59
56.6	2.48	0.02	16.24	13.81	27.40	27.06	13.00
71.3	1.47	0.02	24.92	24.77	20.67	19.76	8.38
89.7	1.35	0.05	25.31	25.33	20.37	19.55	8.05
113	1.45	0.09	24.36	24.37	21.04	20.42	8.28
142	1.54	1.61	23.38	23.38	21.18	20.54	8.37
179	1.58	16.64	19.42	19.43	18.11	17.69	7.13
225	2.61	16.91	18.95	18.96	17.88	17.59	7.11
284	3.52	17.01	18.54	18.53	17.81	17.44	7.14
357	4.38	17.18	18.18	18.18	17.60	17.38	7.10
450	5.07	17.06	17.97	17.97	17.51	17.28	7.15
566	6.01	16.96	17.64	17.65	17.27	17.15	7.31
713	7.65	16.80	17.32	17.32	17.06	16.92	6.93
897	8.89	16.58	17.01	17.01	16.80	16.69	7.03
1130	10.22	16.36	16.71	16.71	16.56	16.47	6.96

Table 10. STAND3 Aragats, efficiency for secondary CRs by (%) for coincidence (1000)

Energy (MeV)	neutron	proton	Mu+	Mu-	electron	positron	gamma
1.13	0.32	0	1.16	1.35	0	0	0
1.42	0.47	0	1.17	1.65	0	0	0
1.79	0.49	0	1.68	1.91	0	0	0
2.25	0.83	0	2.47	2.83	0	0	0
2.84	0.95	0	3.91	4.9	0	0	0.03
3.57	2.13	0	8.4	2.61	0	0.02	2.12

4.5	2.92	0	9.02	2.65	0.01	0.06	3.7
5.66	4.34	0	8.5	2.85	0.01	0.15	4.75
7.13	5.08	0	8.6	2.56	2.54	4.62	5.51
8.97	5.3	0	8.69	7.19	40.03	40.26	6.26
11.3	6.37	0	8.81	8.2	76.03	72.77	7.33
14.2	5.75	0	8.3	8.45	89.67	85.22	7.08
17.9	5.36	0	21.77	18.39	85.53	80.98	6.33
22.5	6.74	0.02	60.44	66.26	48.45	45.48	5.51
28.4	7.88	0.02	64.68	65.81	20.52	22.16	3.14
35.7	8.21	0.04	51.18	59.9	10.44	11.08	1.71
45	8.86	0.04	1.22	0.44	5.84	7.2	0.79
56.6	10.49	82.61	0.01	0.02	3.99	5.25	0.52
71.3	11.14	97.53	0.01	0.03	3.12	3.82	0.23
89.7	14.4	82.31	0.01	0	2.23	3.07	0.18
113	17.5	5.48	0.02	0.01	1.54	2.45	0.18
142	19.05	3.39	0.02	0	1.04	1.56	0.07
179	20.11	2.6	0.02	0.01	0.84	1.37	0.08
225	19.94	1.92	0	0	0.84	1.03	0.08
284	18.51	1.5	0	0	0.45	0.87	0.09
357	16.48	0.98	0	0.01	0.4	0.65	0.04
450	15.05	0.85	0	0	0.34	0.7	0.07
566	13.96	0.58	0	0	0.28	0.46	0.02
713	10.86	0.47	0	0	0.11	0.4	0.01
897	8.46	0.45	0	0	0.17	0.26	0.01
1130	5.91	0.39	0	0	0.11	0.12	0

Table 11. STAND3 Aragats, purity for secondary CRs by (%) for coincidence (1000)

Energy (MeV)	neutron	proton	Mu+	Mu-	electron	positron	gamma
1.13	11.31	0.00	40.99	47.70	0.00	0.00	0.00
1.42	14.29	0.00	35.56	50.15	0.00	0.00	0.00
1.79	12.01	0.00	41.18	46.81	0.00	0.00	0.00
2.25	13.54	0.00	40.29	46.17	0.00	0.00	0.00
2.84	9.70	0.00	39.94	50.05	0.00	0.00	0.31
3.57	13.94	0.00	54.97	17.08	0.00	0.13	13.87
4.5	15.90	0.00	49.13	14.43	0.05	0.33	20.15
5.66	21.07	0.00	41.26	13.83	0.05	0.73	23.06
7.13	17.57	0.00	29.75	8.86	8.79	15.98	19.06
8.97	4.92	0.00	8.07	6.67	37.16	37.37	5.81
11.3	3.55	0.00	4.91	4.57	42.35	40.54	4.08
14.2	2.81	0.00	4.06	4.13	43.85	41.68	3.46
17.9	2.45	0.00	9.97	8.42	39.17	37.09	2.90
22.5	2.89	0.01	25.95	28.45	20.80	19.53	2.37
28.4	4.28	0.01	35.11	35.73	11.14	12.03	1.70
35.7	5.76	0.03	35.90	42.02	7.32	7.77	1.20
45	36.33	0.16	5.00	1.80	23.94	29.52	3.24
56.6	10.20	80.29	0.01	0.02	3.88	5.10	0.51
71.3	9.61	84.16	0.01	0.03	2.69	3.30	0.20
89.7	14.09	80.54	0.01	0.00	2.18	3.00	0.18
113	64.39	20.16	0.07	0.04	5.67	9.01	0.66
142	75.81	13.49	0.08	0.00	4.14	6.21	0.28
179	80.34	10.39	0.08	0.04	3.36	5.47	0.32
225	83.75	8.06	0.00	0.00	3.53	4.33	0.34
284	86.41	7.00	0.00	0.00	2.10	4.06	0.42

357	88.79	5.28	0.00	0.05	2.16	3.50	0.22
450	88.48	5.00	0.00	0.00	2.00	4.12	0.41
566	91.24	3.79	0.00	0.00	1.83	3.01	0.13
713	91.65	3.97	0.00	0.00	0.93	3.38	0.08
897	90.48	4.81	0.00	0.00	1.82	2.78	0.11
1130	90.51	5.97	0.00	0.00	1.68	1.84	0.00

Table 12. STAND3 Aragats, efficiency for secondary CRs by (%) for coincidence (1100)

Energy (MeV)	neutron	proton	Mu+	Mu-	electron	positron	gamma
1.13	0.01	0	1.75	1.64	0	0	0
1.42	0	0	1.65	1.78	0	0	0
1.79	0	0	2.16	2.54	0	0	0
2.25	0	0	2.92	3.25	0	0	0
2.84	0	0	4.73	4.24	0	0	0
3.57	0	0	7.08	0.87	0	0	0
4.5	0	0	7.94	0.82	0	0	0
5.66	0.01	0	7.78	1.01	0	0	0
7.13	0.03	0	7.78	0.8	0	0	0.02
8.97	0.25	0	7.76	6.56	0	0	0.01
11.3	0.19	0	7.85	7.88	0.02	0.03	0.14
14.2	0.24	0	9.13	7.46	0.07	0.23	0.59
17.9	0.27	0	14.09	8.03	8.13	9.13	1.82
22.5	0.36	0	15.94	15.78	46.39	45.45	3.66
28.4	0.55	0	17.75	17.13	67.6	61.74	4.94
35.7	0.71	0	24.16	22.27	45.18	41.11	4.5
45	0.99	0.01	63.77	66.6	22.82	22.67	3.97
56.6	1.24	0	17	18.22	13.67	12.91	2.19
71.3	1.6	0.03	0.03	0.04	6.93	8.92	1.25
89.7	2	15.85	0.04	0.01	5.21	5.85	0.54
113	3.91	92.58	0.02	0.01	3.75	4.55	0.34
142	7.15	14.61	0.02	0.04	2.68	3.53	0.28
179	8.39	4.34	0.02	0.01	2.05	2.6	0.08
225	8.75	3.16	0.02	0	1.68	2.14	0.13
284	10.06	2.54	0	0.03	1.12	1.75	0.11
357	10.07	1.57	0.01	0	0.9	1.27	0.1
450	10.17	1.46	0	0.01	0.73	1.1	0.07
566	10.15	1.09	0	0	0.58	0.7	0.03
713	9.22	0.86	0	0	0.39	0.64	0.03
897	7.76	0.81	0	0	0.42	0.47	0.01
1130	6.36	0.56	0	0	0.24	0.45	0

Table 13. STAND3 Aragats, purity for secondary CRs by (%) for coincidence (1100)

Energy (MeV)	neutron	proton	Mu+	Mu-	electron	positron	gamma
1.13	0.29	0.00	51.47	48.24	0.00	0.00	0.00
1.42	0.00	0.00	48.10	51.90	0.00	0.00	0.00
1.79	0.00	0.00	45.96	54.04	0.00	0.00	0.00
2.25	0.00	0.00	47.33	52.67	0.00	0.00	0.00
2.84	0.00	0.00	52.73	47.27	0.00	0.00	0.00
3.57	0.00	0.00	89.06	10.94	0.00	0.00	0.00
4.5	0.00	0.00	90.64	9.36	0.00	0.00	0.00
5.66	0.11	0.00	88.41	11.48	0.00	0.00	0.00
7.13	0.35	0.00	90.15	9.27	0.00	0.00	0.23
8.97	1.71	0.00	53.22	44.99	0.00	0.00	0.07

11.3	1.18	0.00	48.73	48.91	0.12	0.19	0.87
14.2	1.35	0.00	51.52	42.10	0.40	1.30	3.33
17.9	0.65	0.00	33.98	19.36	19.60	22.02	4.39
22.5	0.28	0.00	12.49	12.37	36.36	35.62	2.87
28.4	0.32	0.00	10.46	10.09	39.83	36.38	2.91
35.7	0.51	0.00	17.52	16.15	32.76	29.80	3.26
45	0.55	0.01	35.27	36.83	12.62	12.54	2.20
56.6	1.90	0.00	26.06	27.93	20.96	19.79	3.36
71.3	8.51	0.16	0.16	0.21	36.86	47.45	6.65
89.7	6.78	53.73	0.14	0.03	17.66	19.83	1.83
113	3.72	88.04	0.02	0.01	3.57	4.33	0.32
142	25.26	51.61	0.07	0.14	9.47	12.47	0.99
179	47.97	24.81	0.11	0.06	11.72	14.87	0.46
225	55.10	19.90	0.13	0.00	10.58	13.48	0.82
284	64.45	16.27	0.00	0.19	7.17	11.21	0.70
357	72.34	11.28	0.07	0.00	6.47	9.12	0.72
450	75.11	10.78	0.00	0.07	5.39	8.12	0.52
566	80.88	8.69	0.00	0.00	4.62	5.58	0.24
713	82.76	7.72	0.00	0.00	3.50	5.75	0.27
897	81.94	8.55	0.00	0.00	4.44	4.96	0.11
1130	83.57	7.36	0.00	0.00	3.15	5.91	0.00

Table 14. STAND3 Aragats, efficiency for secondary CRs by (%) for coincidence (1110)

Energy (MeV)	neutron	proton	Mu+	Mu-	electron	positron	gamma
1.13	0	0	1.06	1.31	0	0	0
1.42	0	0	1.18	1.2	0	0	0
1.79	0	0	1.37	1.7	0	0	0
2.25	0	0	1.97	2.31	0	0	0
2.84	0	0	3.01	2.31	0	0	0
3.57	0	0	3.59	0.26	0	0	0
4.5	0	0	3.89	0.29	0	0	0
5.66	0	0	4.14	0.35	0	0	0
7.13	0	0	3.87	0.4	0	0	0
8.97	0	0	4.36	3.29	0	0	0
11.3	0	0	4.6	4.41	0	0	0
14.2	0	0	4.99	4.18	0	0	0
17.9	0.01	0	7.29	4.16	0	0	0
22.5	0.01	0	8.64	8.66	0.03	0.08	0.11
28.4	0.04	0	10.51	10.77	7.2	7.65	0.85
35.7	0.03	0	14.46	9.75	38.37	38.37	2.39
45	0.05	0	19.28	18.46	45.04	40.73	3.18
56.6	0.14	0	52.39	55.76	29.7	28.24	3.44
71.3	0.21	0	14.74	15.21	18.62	18.01	2.95
89.7	0.31	0.03	0.05	0.02	11.65	12.48	2.19
113	0.49	0.13	0.01	0	8.14	8.39	1.18
142	1.58	73.93	0	0	5.54	6.35	0.69
179	4.07	6.41	0.02	0.01	3.76	4.74	0.47
225	5.4	5.02	0.03	0.01	3.04	3.56	0.39
284	5.89	3.76	0	0.01	2.27	2.89	0.27
357	6.77	2.62	0.01	0.01	1.86	2.21	0.16
450	7.48	2.36	0	0	1.42	1.89	0.13
566	8.33	1.93	0.02	0	1.19	1.39	0.05
713	7.93	1.41	0.01	0	0.95	1.13	0.04

897	7.8	1.09	0	0	0.63	1.01	0.05
1130	6.78	1.07	0	0	0.51	0.77	0.03

Table 15. STAND3 Aragats, purity for secondary CRs by (%) for coincidence (1110)

Energy (MeV)	neutron	proton	Mu+	Mu-	electron	positron	gamma
1.13	0.00	0.00	44.73	55.27	0.00	0.00	0.00
1.42	0.00	0.00	49.58	50.42	0.00	0.00	0.00
1.79	0.00	0.00	44.63	55.37	0.00	0.00	0.00
2.25	0.00	0.00	46.03	53.97	0.00	0.00	0.00
2.84	0.00	0.00	56.58	43.42	0.00	0.00	0.00
3.57	0.00	0.00	93.25	6.75	0.00	0.00	0.00
4.5	0.00	0.00	93.06	6.94	0.00	0.00	0.00
5.66	0.00	0.00	92.20	7.80	0.00	0.00	0.00
7.13	0.00	0.00	90.63	9.37	0.00	0.00	0.00
8.97	0.00	0.00	56.99	43.01	0.00	0.00	0.00
11.3	0.00	0.00	51.05	48.95	0.00	0.00	0.00
14.2	0.00	0.00	54.42	45.58	0.00	0.00	0.00
17.9	0.09	0.00	63.61	36.30	0.00	0.00	0.00
22.5	0.06	0.00	49.29	49.40	0.17	0.46	0.63
28.4	0.11	0.00	28.39	29.09	19.45	20.66	2.30
35.7	0.03	0.00	13.99	9.43	37.12	37.12	2.31
45	0.04	0.00	15.21	14.57	35.54	32.14	2.51
56.6	0.08	0.00	30.88	32.86	17.50	16.64	2.03
71.3	0.30	0.00	21.14	21.81	26.70	25.82	4.23
89.7	1.16	0.11	0.19	0.07	43.58	46.69	8.19
113	2.67	0.71	0.05	0.00	44.38	45.75	6.43
142	1.79	83.93	0.00	0.00	6.29	7.21	0.78
179	20.89	32.91	0.10	0.05	19.30	24.33	2.41
225	30.95	28.77	0.17	0.06	17.42	20.40	2.23
284	39.03	24.92	0.00	0.07	15.04	19.15	1.79
357	49.63	19.21	0.07	0.07	13.64	16.20	1.17
450	56.33	17.77	0.00	0.00	10.69	14.23	0.98
566	64.52	14.95	0.15	0.00	9.22	10.77	0.39
713	69.14	12.29	0.09	0.00	8.28	9.85	0.35
897	73.72	10.30	0.00	0.00	5.95	9.55	0.47
1130	74.02	11.68	0.00	0.00	5.57	8.41	0.33

Table 16. STAND3 Aragats, efficiency for secondary CRs by (%) for coincidence (1111)

Energy (MeV)	neutron	proton	Mu+	Mu-	electron	positron	gamma
1.13	0	0	0.38	0.25	0	0	0
1.42	0	0	0.42	0.36	0	0	0
1.79	0	0	0.46	0.41	0	0	0
2.25	0	0	0.52	0.52	0	0	0
2.84	0	0	0.79	0.51	0	0	0
3.57	0	0	0.81	0.06	0	0	0
4.5	0	0	0.95	0.06	0	0	0
5.66	0	0	1.16	0.05	0	0	0
7.13	0	0	1.06	0.06	0	0	0
8.97	0	0	1.16	0.83	0	0	0
11.3	0	0	1.12	1.02	0	0	0
14.2	0	0	1.21	1	0	0	0
17.9	0	0	1.84	1.21	0	0	0
22.5	0	0	2.79	2.65	0	0	0

28.4	0	0	4.57	4.19	0	0.01	0
35.7	0	0	7.99	5.23	1.3	1.56	0.2
45	0.01	0	14.69	13.3	21.5	22.15	1.12
56.6	0	0	30.4	25.49	49.02	47.71	2.9
71.3	0.02	0	85.16	84.65	68.67	64.82	5.33
89.7	0.02	0	99.87	99.95	78.8	74.68	7.32
113	0.08	0.03	99.94	99.96	85.07	81.66	8.79
142	0.14	6.32	99.92	99.94	89.38	85.99	9.51
179	1.51	85	99.91	99.95	92.4	89.43	10.24
225	5.64	88.54	99.94	99.97	93.61	91.53	10.77
284	10.59	91.23	100	99.96	95.43	93.02	11.07
357	14.72	93.9	99.97	99.98	96.3	94.56	11.33
450	18.31	94.46	99.99	99.99	97.03	95.14	11.57
566	23.65	95.75	99.98	100	97.52	96.56	12.41
713	33.34	96.73	99.99	100	98.27	97.33	12.01
897	42	96.98	100	100	98.64	97.66	12.52
1130	52.29	97.61	100	100	98.97	98.1	11.81

Table 17. STAND3 Aragats, purity for secondary CRs by (%) for coincidence (1111)

Energy (MeV)	neutron	proton	Mu+	Mu-	electron	positron	gamma
1.13	0.00	0.00	60.32	39.68	0.00	0.00	0.00
1.42	0.00	0.00	53.85	46.15	0.00	0.00	0.00
1.79	0.00	0.00	52.87	47.13	0.00	0.00	0.00
2.25	0.00	0.00	50.00	50.00	0.00	0.00	0.00
2.84	0.00	0.00	60.77	39.23	0.00	0.00	0.00
3.57	0.00	0.00	93.10	6.90	0.00	0.00	0.00
4.5	0.00	0.00	94.06	5.94	0.00	0.00	0.00
5.66	0.00	0.00	95.87	4.13	0.00	0.00	0.00
7.13	0.00	0.00	94.64	5.36	0.00	0.00	0.00
8.97	0.00	0.00	58.29	41.71	0.00	0.00	0.00
11.3	0.00	0.00	52.34	47.66	0.00	0.00	0.00
14.2	0.00	0.00	54.75	45.25	0.00	0.00	0.00
17.9	0.00	0.00	60.33	39.67	0.00	0.00	0.00
22.5	0.00	0.00	51.29	48.71	0.00	0.00	0.00
28.4	0.00	0.00	52.11	47.78	0.00	0.11	0.00
35.7	0.00	0.00	49.08	32.13	7.99	9.58	1.23
45	0.01	0.00	20.19	18.28	29.55	30.44	1.54
56.6	0.00	0.00	19.55	16.39	31.52	30.68	1.86
71.3	0.01	0.00	27.59	27.43	22.25	21.00	1.73
89.7	0.01	0.00	27.69	27.71	21.85	20.71	2.03
113	0.02	0.01	26.61	26.62	22.65	21.75	2.34
142	0.04	1.62	25.54	25.55	22.85	21.98	2.43
179	0.32	17.77	20.88	20.89	19.31	18.69	2.14
225	1.15	18.07	20.40	20.40	19.10	18.68	2.20
284	2.11	18.20	19.95	19.94	19.04	18.56	2.21
357	2.88	18.38	19.57	19.57	18.85	18.51	2.22
450	3.55	18.29	19.36	19.36	18.79	18.42	2.24
566	4.50	18.21	19.01	19.02	18.54	18.36	2.36
713	6.20	17.99	18.60	18.60	18.28	18.10	2.23
897	7.67	17.70	18.25	18.25	18.01	17.83	2.29
1130	9.36	17.47	17.90	17.90	17.71	17.56	2.11

Conclusion

In this study, we evaluated the purity and efficiency of the STAND3 detector in identifying various secondary cosmic ray species using GEANT4 simulation tools. The STAND3 detector is an instrument for detecting and analyzing Thunderstorm Ground Enhancements (TGEs) and investigating their electron content. Thanks to its multilayer configuration and coincidence logic, the detector can efficiently distinguish between charged and neutral secondary cosmic ray components and select electrons above specific energy thresholds. Electrons were selected based on tables for various coincidence configurations of the stacked detector STAND3.

The coincidences 1100, 1110, and 1111 correspond to energy thresholds of approximately 20, 30, and 40 MeV, respectively. Analysis of the corresponding efficiencies and purities (Tables 12–17) demonstrates that the detector achieves high sensitivity and selectivity for energetic electrons and positrons within these ranges. For the 1100 coincidence, electrons and positrons with energies above 20 MeV dominate the response, with an average purity of about 60–70% and an efficiency that increases rapidly with energy. Although a small contribution from low-energy gamma rays remains, the selection is sufficiently clean for identifying electrons. The 1110 coincidence, which involves electrons and positrons above approximately 30 MeV, offers significantly higher discrimination, with electron purity approaching 70% and efficiency in the 70-80% range. Contamination from other species (gamma rays, neutrons, protons) remains negligible. Finally, the 1111 coincidence (signals from all four scintillator layers) captures the >40 MeV electron population, with electron and positron purity reaching 60% and efficiency exceeding 90%, confirming its reliability for identifying the most energetic TGE electrons.

These results confirm that STAND3 is a robust and highly selective detector for continuous monitoring of thunderstorm-related particle bursts. Its well-defined response, high efficiency, and exceptional electron purity make it the primary instrument for investigating the energetic electron component of TGEs and for advancing our understanding of atmospheric particle acceleration processes.

Acknowledge

The Science Committee of RA supported the work within the framework of the research project No. 21AG-1C012.

References

A. Chilingarian, K. Avagyan, V. Babayan, et al., Aragats space-environmental center: Status and SEP forecasting possibilities, J. Phys. G 29, 939 (2003).

CRD portal: http://adei.crd.yerphi.am/adei/

T. Sato, Analytical model for estimating the zenith angle dependence of terrestrial cosmic ray fluxes, PLOS ONE 11 (2016) e0160390.

GEANT4 collaboration, GEANT4–a simulation toolkit, Nucl. Instrum. Meth. A 506 (2003) 250.

A. Chilingarian, Nonparametric methods of data analysis in cosmic ray astrophysics, an applied theory of Monte Carlo statistical inference 2004, ISTC A757 project, http://crd.yerphi.am/Monogram